# Density functional studies of small silicon clusters adsorbed on graphite (0001) and diamond (100)

J. H. Wu and F. Hagelberg
*Computational Center for Molecular Structure and Interactions, Department of Physics, Atmospheric Sciences, and General Science, Jackson State University, Jackson, Mississippi 39217, USA*
(Received 21 May 2007; published 11 October 2007)

The structural and electronic properties of small silicon clusters ($Si_n$ with $n=2-7$) adsorbed on graphite (0001) and diamond (100) substrates are studied by density functional theory within periodic boundary conditions. A three-layer graphene slab with 60 carbon atoms in each layer is used to represent the graphite substrate. The diamond substrate is described by an eight-layer slab involving a $p(8\times4)$ surface cell. Side adsorption geometry of $Si_n$ on the substrates is considered. Maximum stability is encountered for particle site adsorption of the $Si_n$ clusters on the graphite surface and for bridge site adsorption on diamond. Weak covalent interaction prevails between the cluster and the graphite substrate, while much stronger bonding effects are observed for adsorption on diamond, leading to considerable structural deformation of the cluster. Partial density of states distributions are calculated for the $Si_n$ adsorbates. From this analysis, the clusters exhibit a distinct narrowing of their energy gaps upon deposition on the surfaces. This effect is found to be weak for the graphite and very substantial for the diamond substrate. In the latter case, it is attributed to the emergence of spectral lines close the Fermi energy of the cluster-substrate composite, reflecting sizable interaction between the *p*-electron subsystems of $Si_n$ and diamond.

DOI: 10.1103/PhysRevB.76.155409 PACS number(s): 73.20.Hb, 68.43.Bc, 36.40.Cg

## I. INTRODUCTION

The field of nanoscience has seen an explosive development during the past decade. The objective of nanoscience and nanotechnology is to understand, control, and manipulate the behavior of objects at the nanometer scale. Silicon clusters ($Si_n$) and silicon nanostructures are widely studied for their fundamental role in cluster physics and chemistry as well as their applications in materials science.[1–5] The optical and electronic properties of these nanosystems are largely governed by the quantum size effect. Thus, the size dependence of the energy gap between the highest occupied molecular orbital and the lowest unoccupied molecular orbital is essential for understanding the material properties of these systems, such as intrinsic conductivity and optical transitions.

For experimental investigation of their properties, pure clusters are generally deposited on a substrate. The interaction between the clusters and the substrate affects the cluster as well as the substrate. As documented by a large number of experimental and theoretical studies on pure graphite and on clusters adsorbed on the graphite surface, the latter provides a particularly important substrate for cluster deposition. This is related to its planar geometry and weak van der Waals interlayer coupling which make it possible to split flat, clean surfaces. These are ideal for studying the adsorption of surface layers and clusters.

In a recent experiment, pristine Si clusters were grown on highly oriented pyrolytic graphite upon submonolayer deposition of Si atoms.[6] Scanning tunneling microscopy was used to determine the $Si_n$ cluster energy gaps. The experimental results reflect a reversal of the commonly assumed trend of an energy gap increase as one goes from the infinite bulk to finite cluster systems. For all experimentally observed $Si_n$ diameters, the measured energy gaps turned out to be sizably smaller than that of bulk silicon (1.1 eV). For smaller cluster diameters, the largest recorded gap amounts to 0.45 eV. This experimentally observed trend of $Si_n$ energy gap narrowing upon deposition on a graphite substrate was recently confirmed by investigating the smallest $Si_n$ cluster, $Si_3$, on the basis of density functional theory (DFT) within periodic boundary conditions.[7] DFT studies on both $Si_2$ and $Si_3$ on graphite yielded a tendency of the Si cluster constituents to locate close to particle sites of the graphite surface, resulting in a structural adjustment of the adsorbate.

Diamond has been widely utilized as a constituent of a large variety of devices, such as field effect transistors, elements of high power electronics, coating, and cutting tools.[8] This preference is related to its unique mechanical, thermal, electrical, and optical properties. In terms of nanoscience, the observation that clusters adhere strongly to the diamond substrate is particularly relevant. The (100) surface of diamond is unique because each surface atom has two dangling bonds while only a single dangling bond per atom is found at the (111) and (110) surfaces, making the surface chemistry of the (100) prototype much richer than that of the latter two alternatives. Theoretical studies of the clean diamond $(100)-2\times1$ systems have revealed reorganization of the C surface atoms into dimer substructures.[9] The reconstruction of the (100) diamond surface leads to formation of rows of symmetric dimers with a bond length of $d=1.38$ Å (Fig. 2).

In this contribution, we present a comparative study of $Si_n$ cluster adsorption on graphite and diamond substrates. These systems are modeled by use of density functional theory within periodic boundary conditions. In the following, we outline the computational details of this work. Subsequently, we present and discuss the calculated results. Finally, we add some concluding remarks.

 

## II. COMPUTATIONAL DETAILS

The calculations have been performed using the Vienna *ab initio* simulation package,[10,11] which is based on DFT.[12] More specifically, the finite temperature version of local density functional (LDF) theory, as developed by Mermin,[13] is utilized in conjunction with the exchange-correlation functional given by Ceperley and Alder and parametrized by Perdew and Zunger.[14] Finite temperature LDF theory introduces a smearing of the one-electron levels and helps to solve convergence problems arising from the use of small sets of $k$ points for Brillouin-zone integrations.[15] The generalized Kohn-Sham equations[12] are solved employing a residual minimization scheme, namely, the direct inversion in the iterative subspace method.[16,17] The optimization of the atomic geometry is performed via conjugate-gradient minimization of the total energy with respect to the atomic coordinates.

The interaction of valence electrons and core ions is treated by the projector-augmented wave method.[18] The Perdew-Burke-Ernzerhof[19] type generalized gradient correction (GGA) for the exchange-correlation functional was used for the adsorption of the diamond substrate.

All systems involving the graphite substrate, however, were described by use of the LDA exchange-correlation functional. The rationale for employing the LDA approach in these cases was the observation that the GGA fails to account for the weak van der Waals-type interaction between the graphite layers.[20,21] In fact, this interaction is predicted to be repulsive by the GGA approach, such that the graphite layers are not seen to cohere at all if the latter method is used to describe them. Recently, the GGA potential was extended by a semiempirical term to improve its treatment of van der Waals effects.[22] This correction was employed in the study of molecular adsorbates on graphite.[22] The obtained equilibrium structures and adsorption energies were found to be closer to the LDA than to the GGA results.

For comparison of the LDA and GGA methods with reference to the systems discussed in the present context, we treated $Si_5$ as a test system adsorbed on the diamond substrate with both procedures. The difference of the corresponding bond lengths of the final structures obtained from LDA and GGA is less than 2%. However, the LDA adsorption energy is 1.1 eV higher than the respective GGA result.

The substrates are modeled by slabs within three-dimensional periodic boundary conditions. Due to weak interlayer bonding, it is sufficient to represent the graphite substrate by three graphene layers, which are fully optimized and arranged according to the *ABA* stacking scheme. In order to minimize the interaction between neighboring cluster adsorbates, a $12.23\times12.71\times26.71$ Å$^3$ supercell (TTTC), consisting of 60 carbon atoms was used to model the graphene layer [Fig. 1(a)]. In total, our description of the graphite substrate involves 180 carbon atoms. Two neighboring slabs are separated by a space of more than 20 Å of vacuum. An eight-layer slab, separated by a 11.6 Å vacuum region, is used to model the diamond C(100) substrate. It was verified that increasing the thickness of the slab from 8 to 16 layers did not change the energy of the surface states by more than a few meV.[9] Two bottom layers of the diamond slab are fixed at the geometric parameters characteristic for the bulk system, where the bulk lattice constant is calculated to be 3.564 Å. As shown by a test calculation reported in Ref. 9, constraining the bottom layers induces negligibly small energy shifts of the surface states. For the diamond substrate, we used a $p(8\times4)$ surface cell composed of 32 atoms per layer with a total of 256 C atoms (Fig. 2). The cell size is kept constant during geometry optimization.

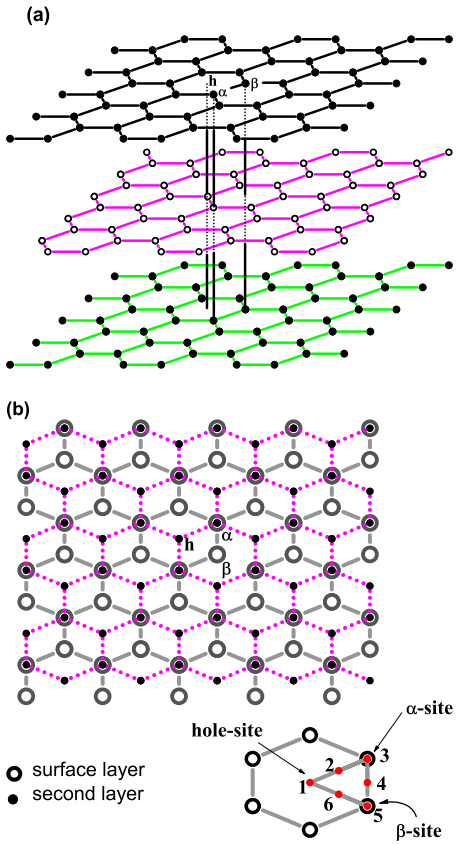


FIG. 1. (Color online) Schematic representation of the graphite substrate. (a) Side view and (b) top view. The highly symmetric sites-$\alpha$, $\beta$, and hole sites (h) are indicated.

The equilibrium geometries of the $Si_n$ clusters and the substrate have been obtained by subjecting the composite of slab and adsorbed cluster to total energy optimization.

The definition of the adsorption energy is

$$E_{adsorp} = E_{slab} + E_{cluster} - E_{composite}, \quad (1)$$

where $E_{slab}$ and $E_{cluster}$ denote the total energies of the free substrate and the free $Si_n$ cluster, respectively, while $E_{composite}$ stands for the total energy of the combined system of the $Si_n$ cluster and the substrate.

In order to obtain accurate adsorption energy results, we utilize the same parameters for all calculations. These involve an energy cutoff $E_{cut}$=400 eV for the plane wave functions and a smearing width of $\sigma$=0.01 eV to parametrize the finite temperature LDF. As we increase the energy cutoff to $E_{cut}$=800 eV, the geometry of our test system $Si_3$ and $Si_5$ on both substrates, graphite and diamond, does not change in comparison with $E_{cut}$=400 eV, and the deviation in adsorption energy is in the order of meV. Reduction of $\sigma$ to

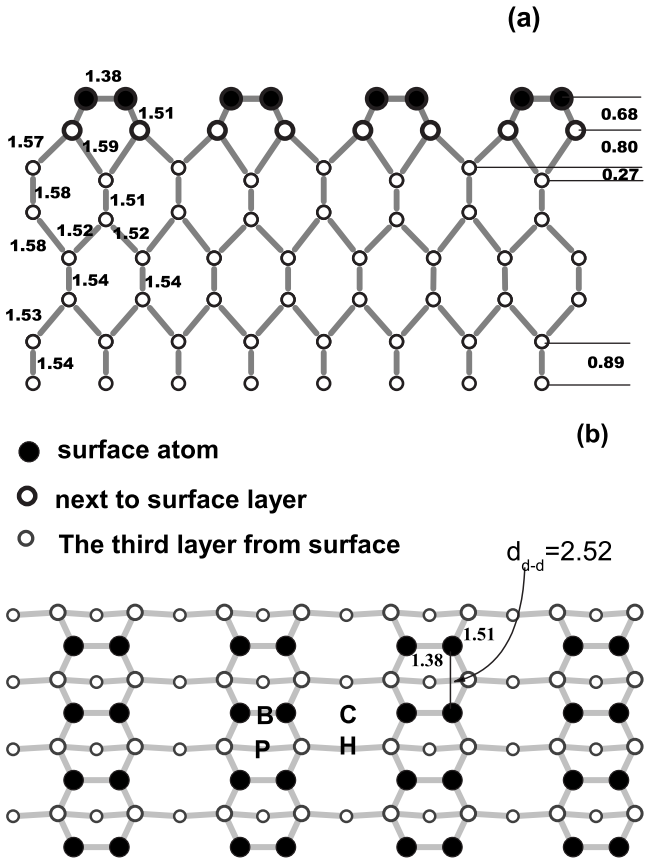


FIG. 2. (2×1) reconstruction of the diamond substrate. (a) Side view and (b) top view, with P being the pedestal site, B the bridge site, C the cave site, and H the hollow site.

0.0001 eV results in a total energy variation of less than 1 meV as compared with the choice $\sigma$=0.01 eV. Further, the partial occupancies of each wave function are defined by use of the tetrahedron method with Blöchl corrections.[23]

## III. RESULTS AND DISCUSSIONS

Before discussing composites of $Si_n$ adsorbates and graphite or diamond substrates, we examine the properties of the respective pure surfaces in Sec. III A. The following subsection focuses on single Si atom adsorption on both graphite and diamond in preparation of our treatment of Si cluster-substrate interaction in the remaining segments of this section. Adsorption of $Si_n$ ($n$=3–7) on graphite is discussed in Secs. III C–III E while Sec. III F deals with $Si_n$ ($n$=2–7) on diamond. The two concluding subsections address the change of the $Si_n$ energy gap upon cluster deposition on graphite or diamond (Sec. III G) and the reorganization of the electron charge density of either substrate as a consequence of $Si_n$ adsorption (Sec. III H).

### A. Graphite and diamond substrates

The graphite substrate is represented by a three-layer slab with all atomic positions left free to vary during optimization. The results of this calculation demonstrate that the structure of the slab deviates only marginally from that of the bulk. The surface energy amounts to $\sigma_{ene}$=0.283 eV within the TTTC. As 60 atoms are included in each layer, the surface energy per atom is found to be about 0.005 eV. This is lower than the respective result for the surface energy of the $p(3\times3)$ surface cell[7] (0.023 eV/surface atom). This finding confirms that graphite can be treated as a two-dimensional system due to weak interlayer interaction.

The structure of the reconstructed diamond surface was found to be near identical with that reported in Ref. 9. The symmetric dimer exhibits a bond length of $d_{dimer}$=1.38 Å, which is slightly larger than that reported in Ref. 9 ($d_{dimer}$ =1.37 Å) (Fig. 2). The bond length deviations do not exceed 2%, although different choices for both the pseudopotentials and the surface cells were made in the two compared computations. The distance between two neighboring dimers in the row is $d_{d-d}$=2.52 Å. For a detailed discussion of the (2×1) reconstructed diamond surface, the reader is referred to the work of Furthmüller *et al.*[9]

We further confirmed that for both supercells employed here, i.e., a 12.23×12.71×26.71 Å$^3$, (TTTC) and an 8×4 model for the graphite and the diamond substrates, respectively, the interaction of neighboring clusters is minimal. As a test, we compared the total energy results for $Si_5$ on graphite and diamond, employing the TTTC and the 8×4 supercell, with that obtained by using a further supercell of dimension 20×20×20 Å$^3$. For both the graphite and the diamond substrate, the respective energy difference was found to be within a few meV.

### B. Single atom adsorption

In order to map the potential energy surface for single Si atom adsorption on graphite and diamond substrates we have considered various initial locations of the Si atom above both surfaces [Figs. 1(b) and 2(b)]. Six Si atom sites on graphite are examined, as shown in Fig. 1(b). The respective findings are compared with our previous results related to Si atoms on the same substrate. Four Si atom sites are distinguished on the diamond surface [Fig. 2(b)].

For a given substrate, the total energy of the studied composites is used to compare different Si adsorption sites with respect to stability. Table I lists the results of these computations. They suggest that the potential energy surface of Si adsorbed on graphite is found to be slightly flatter within the TTTC than that within the $p(3\times3)$ surface cell. The largest differences in adsorption energy are 0.381 and 0.432 eV for the TTTC and the $p(3\times3)$ surface cell, respectively. However, the stability order of the adsorption for different sites is the same for these two supercells. As previously observed,[7] the hole site [site 1 in Fig. 1(b)] is not favored for Si adsorption on the graphite substrate. This is rationalized by the tendency of the Si atom to form covalent bonds with C, combined with the fact that the hole site is deprived of electronic charge density, and thus involves naturally the least charge density overlap between the Si adsorbate and C substrate atoms. Among the remaining five Si adsorption sites, the potential energy varies little. The largest difference between adsorption energies is less than 100 meV. From this

TABLE I. The adsorption energy of a single Si atom attached to the graphite and diamond substrates with different initial locations. All energies are in eV.

| | Site | 1 | 2 | 3 | 4 | 5 | 6 |
|---|---|---|---|---|---|---|---|
| Graphite | TTTC | 1.387 | 1.768 | 1.684 | 1.726 | 1.676 | 1.734 |
| | $p(3\times3)$ | 1.369 | 1.801 | 1.639 | 1.748 | 1.645 | 1.784 |
| Diamond | Site | P | H | B | C | | |
| | $p(8\times4)$ | 4.381 | 3.472 | 5.050 | 3.850 | | |

study, the $p(3\times3)$ surface cell is found to be sufficiently large to study single Si atom adsorption on the graphite substrate which justifies the methodology used in our previous treatment of this problem.[7]

In contrast to the adsorption of Ti atoms on diamond,[25] the most stable site of Si adsorbed on diamond is the bridge site, involving a Si atom located above the midpoint of a C dimer on the reconstructed surface. For this structure, the adsorption energy amounts to 5.050 eV which exceeds that found for the analogous configuration on the graphite substrate by a large margin. At the hollow site [H in Fig. 2(b)], involving a Si atom above the center of a square formed by four neighboring dimer atoms of the reconstructed diamond surface, the adsorption energy is 3.472 eV. The comparison between our finding for the bridge and the hollow site demonstrates that the potential energy surface for atomic Si attached to the (100) diamond surface is characterized by sizable variations.

With respect to geometric reconstruction of the surface, Si adsorbed on the bridge site exerts some influence on the dimer substructures of diamond. In particular, the dimer bond length is found to be increased from 1.38 to 1.63 Å as a result of single Si atom adsorption.

As mentioned above, the Si atom forms covalent bonds with the C atoms of the graphite surface. The same bonding principle is realized for diamond as substrate. Therefore, the site with the highest charge density will be the preferred site for Si atom adsorption on both graphite and diamond. This behavior differs characteristically from Na adsorption on graphite[24] and Ti adsorption on diamond.[25] In the first case, ionic bonds are formed between metal and C atoms on account of electron transfer from the adsorbate to the substrate. Accordingly, the hole sites are the favored places of attachment. In the second case, the pedestal site [see Fig. 2(b)] is preferred, since it involves four dangling bonds, matching the valence of the Ti atom and resulting in strong cohesion between substrate and adsorbate.

The other two possible adsorption sites [D1 and D2 in Fig. 2(b)], involving particle positions on the C-C dimer, are unstable. A single Si atom attached to these sites moves to the bridge site in the course of geometry optimization.

### C. $Si_3$ on the graphite substrate

For $Si_3$ adsorbed on graphite, two structural prototypes were identified. The first one involves strong interaction between the substrate and the adsorbate (see Ref. 7). Here, the cluster deforms to accommodate to the potential energy surface of a Si atom in contact with graphite, as described in the preceding subsection. The alternative configuration preserves the $Si_3$ equilibrium geometry. In this case, the cluster interacts weakly with the surface to which it is loosely attached.

In both cases, $\beta$ site adsorption, involving all three Si atoms positioned at places above the $\beta$ sites of the graphite surface or close to these places, turns out to be of maximum stability. In the following discussion of the two basic adsorption geometries, we will therefore focus on the $\beta$ site. In contrast to the adsorption of a single Si atom, for $Si_3$ clusters, we note a sensitivity of the results to the surface cell used, $p(3\times3)$ or TTTC. If the former is employed, bonding between individual Si cluster constituents and C atoms of the surface determines the equilibrium geometry. Utilizing the latter, however, we find that the alternative configuration of an intact $Si_3$ unit that attaches weakly to the surface is favored. Since both results are obtained under identical conditions, except for the supercell size, the difference in geometries may be ascribed to a mutual interaction between neighboring $Si_3$ clusters which is present in the case of the $p(3\times3)$ and absent, or negligibly small, for the TTTC. As the latter supercell is chosen, however, the deformed structure is only by 0.03 eV higher in total energy higher than the most stable structure.

The interaction energy between neighboring clusters can be obtained by subtracting the total energy as evaluated for the larger cell (TTTC) from that found for the smaller $p(3\times3)$. This interaction energy turns out to be 0.094 eV for the intact and 0.142 eV for the deformed $Si_3$ cluster in the $p(3\times3)$ surface cell. The resulting interaction energy difference between the intact and the deformed alternative is thus about 0.05 eV for the $p(3\times3)$ surface cell, which exceeds the difference (0.03 eV) between the total energies obtained for these two situations adopting the TTTC. We conclude from this finding that the neighboring clusters stabilize the deformed $Si_3$ structure more strongly than the intact one if the $p(3\times3)$ supercell is chosen to describe the system.

If the TTTC is adopted, the intact $Si_3$ adsorbate results with lower total energy than the deformed one. The $\beta$ site adsorption energy for the deformed cluster, however, exceeds that for the intact one, the former being 0.759 eV, the latter 0.388 eV. Here, $E_{cluster}$ in Eq. (1) is defined by the energy of the deformed cluster.

### D. $Si_4$ on the graphite substrate

The ground state structure of $Si_4$ is that of a planar rhombus.[27] The $Si_4$ cluster is placed on the graphite substrate

TABLE II. Adsorption energy (eV) of $Si_n$ ($n=3-7$) attached to graphite and diamond substrates with different initial locations.

| Substrate | Graphite | | | Diamond |
|---|---|---|---|---|
| Site | $\alpha$ | $\beta$ | Hole | Bridge |
| $Si_3$ | 0.368 | 0.388 | 0.308 | 5.186 |
| $Si_4$ | 0.603 | 0.607 | 0.446 | 4.965 |
| $Si_5$ | 0.350 | 0.351 | 0.331 | 3.960 |
| $Si_6$ | 0.372 | 0.365 | 0.353 | 4.056 |
| $Si_7$ | 0.380 | 0.385 | 0.368 | 3.245 |

with its plane parallel to the surface. Three surface locations of the Si atoms above the graphite surface were considered as initial locations of the $Si_4$ cluster. More specifically, all the Si atoms were located initially near $\alpha$, $\beta$, and hole sites of the graphite surface, where the interatomic distances of the four Si atoms were chosen in accordance with the $Si_4$ gas phase equilibrium structure. The final geometries were obtained by allowing for geometric relaxation of the combined system. In all cases considered, the $Si_4$ cluster was found to maintain its structure and to adsorb above the graphite substrate with a distance of about 3.10 Å for $\alpha$ and $\beta$ sites, and 3.30 Å for the hole site. The difference of the adsorption energies between $\alpha$ and $\beta$ sites is very small, namely, 0.004 eV (see Table II). However, the adsorption energy of the hole site is less by about 0.16 eV than that obtained for the $\alpha$ and $\beta$ sites. This is consistent with the above results on single Si atom adsorption on graphite, as the hole site exhibits a marked deviation from the otherwise rather flat potential energy surface of a Si atom adsorbed on the graphite substrate.

In order to map the potential energy surface for a $Si_4$ cluster in contact with the graphite surface, we performed an energy scan in vertical direction by systematically varying the position of $Si_4$ with respect to the surface but preserving the surface parallel orientation of the cluster. The vertical distance between the planes of $Si_4$ and graphite was changed from 3.4 to 2.4 Å with a step size of 0.05 Å as three different lateral positions for $Si_4$ are chosen, namely, with the four Si atoms located near $\alpha$, $\beta$, and hole sites (Fig. 3). This computation confirms 3.10 and 3.30 Å as vertical distances $d_z$ of lowest energy for $\alpha/\beta$ and hole adsorption, respectively. The energy increases quickly as $d_z$ decreases and slowly as $d_z$ increases from the equilibrium distance. The difference between the adsorption energies at $\alpha$ and $\beta$ sites is small, while the hole site adsorption energy gradually approaches that for $\alpha$ and $\beta$ site adsorption from above as $d_z$ increases. The condition $\Delta E \equiv E - E_{substrate} - E_{cluster} = 0$ defines the transition from attractive to repulsive interaction between $Si_4$ and the graphite substrate. Thus, the regimes $d_z < 2.58$ Å and $d_z < 2.84$ Å are repulsive for $\alpha/\beta$ and for hole site adsorption, respectively.

In the case of $\alpha/\beta$ site adsorption, the cluster-substrate interaction may be attributed to weak covalent effects between the $Si_4$ unit and the graphite surface layer. This effect is illustrated in Figs. 4(a) and 4(b) which displays the electron charge density of the $Si_4$-graphite composite at equilibrium geometry in an isosurface representation. Figure 4(b) documents a distinctly enhanced electron charge density between the cluster and the adjacent graphite layer, corresponding to the overlap of cluster and surface $\pi$ electron states, extending perpendicularly to the plane of $Si_4$ and to that of the graphite layer. A comparative discussion of adsorbate-substrate interaction for both graphite and diamond in terms of the electron charge density is presented in Sec. III H.

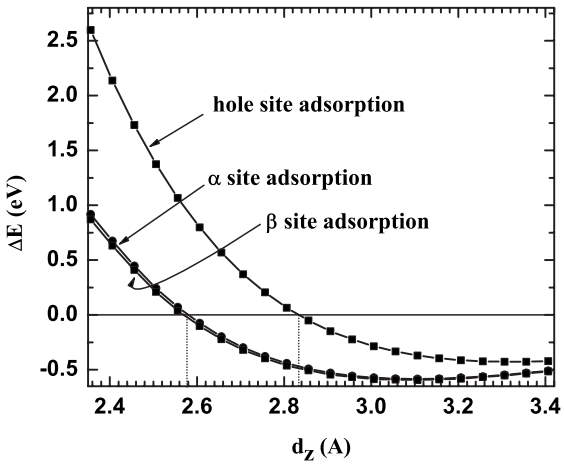


FIG. 3. Adsorption energy of $Si_4$ on graphite as a function of the vertical distance from the surface for three different adsorption sites.

### E. $Si_n$ ($n=5-7$) adsorbed on the graphite substrate

The clusters $Si_5$, $Si_6$, and $Si_7$ are three dimensional, realizing trigonal, tetragonal, and pentagonal bipyramid structures in the gas phase.[26] For each unit, a broad variety of adsorption geometries is conceivable. In the context of this work, we consider configurations that involve surface parallel orientation of a cluster plane to the graphite surface in order to maximize the contact between Si atoms of the cluster and C atoms of the substrate. For $Si_5$ and $Si_6$, we analyzed in addition the case of edge adsorption, where two Si atoms interact with the graphite surface. If this configuration is realized, the total energy for $Si_5$ ($Si_6$) is found to be about 0.10 eV (0.20 eV) higher than that for plane adsorption.

Proceeding as in the cases of $Si_3$ and $Si_4$, we defined the initial cluster locations by placing Si atoms above three characteristic surface sites. That is, the three Si atoms with the smallest vertical distance from the surface are located near $\alpha$,

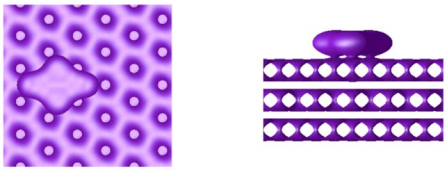

FIG. 4. (Color online) Isosurface map of $Si_4$ on graphite at equilibrium geometry. (a) Top view and (b) side view, demonstrating upbuild of $\pi$ electron charge density in the space between surface and cluster.

$\beta$, and hole sites of the graphite surface. From these calculations, it is seen that $Si_n$ ($n$=5, 6, and 7) clusters tend to keep their structures, and adsorb above the graphite substrate with a distance of about 3.30 Å for $\alpha$, $\beta$, and hole sites. For the three configurations, the adsorption energy varies between 0.330 and 0.385 eV as one goes from $Si_5$ to $Si_7$, where hole site adsorption is found to be about 0.02 eV less stable than $\alpha/\beta$ site adsorption. From this comparison, the potential energy surface for the attachment of $Si_n$ ($n$=5, 6, and 7) to graphite is flatter than that for $Si_3$ and $Si_4$ adsorption, allowing for facile lateral motion of the adsorbed species.

### F. $Si_n$ ($n$=2–7) adsorbed on a diamond substrate

As discussed above, the Si atom interacts strongly with the diamond substrate. The maximum adsorption energy for a single Si atom was found at a bridge site (5.05 eV). From Table I, this site is strongly preferred over alternative positions, reflecting sizable variation of the potential energy surface for Si attached to the diamond surface. While the bond length of the gas phase $Si_2$ cluster is 2.25 Å, the distance between nearest neighboring bridge sites is $d_{d-d}$=2.52 Å [see Fig. 2(b)]. Consequently, the bond length of the $Si_2$ cluster adsorbed to diamond is elongated, with the Si-Si distance increased to 2.48 Å. In addition, the interatomic distance of the carbon dimer on the reconstructed diamond surface is elongated from 1.38 to 1.72 Å upon $Si_2$ adsorption. This indicates that the interaction between the two C atoms of the reconstructed dimer is weaker in the presence of $Si_2$ than in the case of the free surface.

The vertical distance between the $Si_2$ cluster and the diamond surface is 1.81 Å. The C-C dimers interacting with $Si_2$ move toward the adsorbate. The vertical displacement is 0.11 Å as compared to the dimers not in contact with $Si_2$. The Si-C bond length is 1.90 Å,[28] and thus the same as that of the C-Si single bond in the $CSi_4H_{12}$ molecule. This suggests that a single bond is formed between the C and Si atoms. The adsorption energy is found to be 6.10 eV and thus lower than that of two separated Si atoms adsorbed on the bridge site of the diamond surface (10.11 eV), but much higher than that of $Si_2$ adsorbed on $\beta$ sites of the graphite surface (1.43 eV).

The adsorption of $Si_n$ ($n$=3–7) clusters on the diamond substrate was investigated for the case of planar cluster adsorption. Two of the three Si atoms closest to the substrate are positioned initially in the neighborhood of bridge sites and the remaining Si atom is placed close to the cave site (see Fig. 2). From geometry optimization, we obtain $Si_3$ cluster bond lengths of $d_{I-III}$=2.25 Å, $d_{I-II}$=2.53 Å, and $d_{II-III}$ =2.80 Å, which differ markedly from those of the free $Si_3$ cluster (2.20, 2.20, and 2.85 Å). The strong interaction between Si atoms and C atoms causes the distance of Si (I) and Si (II) (see Fig. 5) to increase in order to match the distance between two parallel carbon dimers (dimers 12 and 34 in Fig. 5). The vertical distance between the $Si_3$ cluster and the diamond surface is 1.92 Å. The carbon atoms that interact with $Si_3$ move toward the cluster. With reference to Fig. 5, the bond length of the dimer composed of atoms C(1) and C(2) stretches from 1.38 to 1.75 Å. This is ascribed to the impact of the two Si atoms (I, III) interacting with the dimer. The distance between the constituents C(3) and C(4) of the adjacent dimer which is in contact with a single Si atom (II) increases only to 1.60 Å. The adsorption energy is 5.19 eV and thus about 0.9 eV lower than that found for the adsorption of a $Si_2$ cluster on diamond and much higher than that for the analogous situation involving graphite (0.39 eV).

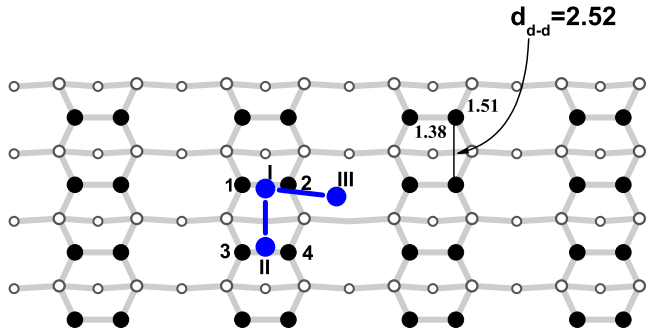


FIG. 5. (Color online) Top view of the initial location of the $Si_3$ cluster adsorbed on diamond substrate.

The adsorption of $Si_4$ on diamond is calculated for two cases: (a) two Si atoms initially located near bridge sites, and the other two near cave sites (see Fig. 6) (b) four Si atoms initially located near hollow sites (see Fig. 2). The first configuration turned out to be of higher stability than the second. We thus restrict the following discussion to the first alternative. The $Si_4$ cluster almost retains its planar rhombic shape as it adsorbs to the diamond substrate. The deformation angle, measuring the deviation from planarity is 0.730°. The rhombic structure, however, is deformed. The four bond lengths of the $Si_4$ cluster elongate from 2.33 Å to $d_{III-IV}$ =2.44, $d_{I-II}$=2.48, $d_{II-III}$=2.50, and $d_{I-IV}$=2.57 Å. Further, upon geometry optimization, the orientation of $Si_4$ is not parallel to the surface any longer. It exhibits a tilt with respect to the surface plane of about 6.70°. The two Si atoms initially placed near the cave sites [(III) and (IV) in Fig. 6] move closer to the diamond surface during optimization. The bond lengths of the carbon dimers in contact with a Si atom increase from 1.38 Å to $d_{3-4}$=1.85 Å and $d_{1-2}$=2.04 Å. The adsorption energy is 4.97 eV which is slightly lower than that found for $Si_3$ on diamond but exceeds that of $Si_4$ adsorbed on graphite by 4.36 eV.

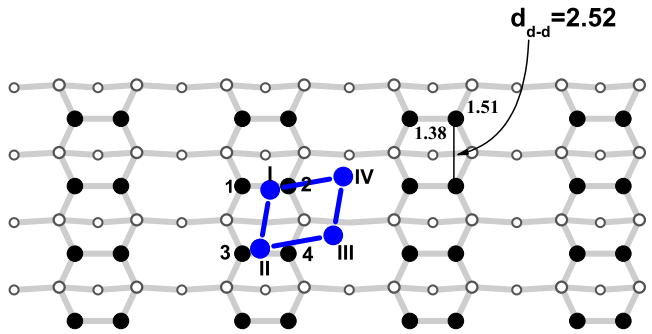


FIG. 6. (Color online) Top view of the initial location of the $Si_4$ cluster adsorbed on diamond.

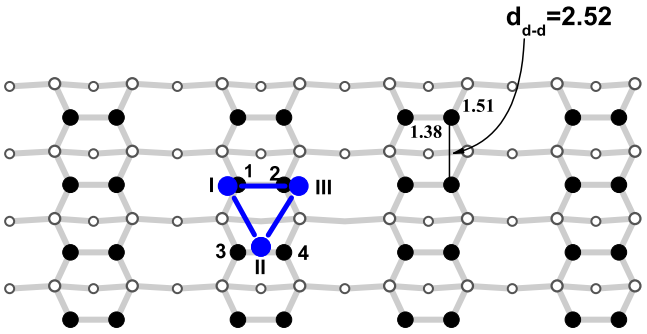


FIG. 7. (Color online) Equilibrium structure of the $Si_n$ ($n=5-7$) in contact with diamond.

For $Si_5$, $Si_6$, and $Si_7$ on diamond, the initial orientation of the clusters is the same as in the case of adsorption on graphite. The initial locations of the three Si atoms in contact with the surface are similar to those of $Si_3$ adsorbed on the diamond substrate (Fig. 5). The strong interaction between Si clusters and the diamond surface deforms the clusters. Two of the three Si atoms attached to the surface move to the dimer sites, as shown in Fig. 7, while the third Si atom remains on the bridge site. The bond lengths of the carbon dimers elongate from 1.38 Å to around 1.65 Å for $Si_n$ ($n=5-7$) adsorption. This is about 0.1 Å longer than the C-C bond length in ethane. The interaction between the constituents of the reconstructed carbon dimer becomes weaker as the silicon clusters are adsorbed on the diamond substrate. The adsorption energies for $Si_5$ and $Si_6$ are close to 4.0 eV, and by 0.75 eV lower for $Si_7$ adsorption (Table II).

### G. Energy gaps of deposited $Si_n$ ($n=3-7$) clusters

In what follows, we comment on the energy gaps of the considered $Si_n$-graphite and $Si_n$-diamond composites, as obtained by density of states (DOS) computations. Previously, it has been shown by calculations based on the $p(3\times3)$ surface cell[7] that the energy gap of graphite narrows as a consequence of the interaction between the graphite surface and atomic as well as molecular ($Si_2$, $Si_3$) Si adsorbates. Adopting the TTTC, it was observed that the $Si_3$ cluster remains largely intact. What statement can be made about the energy gap in this case?

We employ two procedures to address this question. The first is the difference method[7] where the DOS of $Si_3$ is generated by subtracting the DOS of the pure graphite substrate from that of the $Si_3$-graphite composite. The second procedure involves computing the partial density of states (PDOS) for $Si_3$ as part of the combined system, and summing over all contributions thus obtained. Figure 8 contains the DOS of the equilibrium $Si_3$ cluster and of the $Si_3$ adsorbate according to both the PDOS and the difference method computation. The comparison between Figs. 8(b) and 8(c) demonstrates that the PDOS of the $Si_3$ components is smoother than the result of the difference method. The peaks appear at the same positions, irrespective of the applied procedure. Both methods are thus in good agreement. The two distributions for deposited $Si_3$ show well defined peaks whose positions are

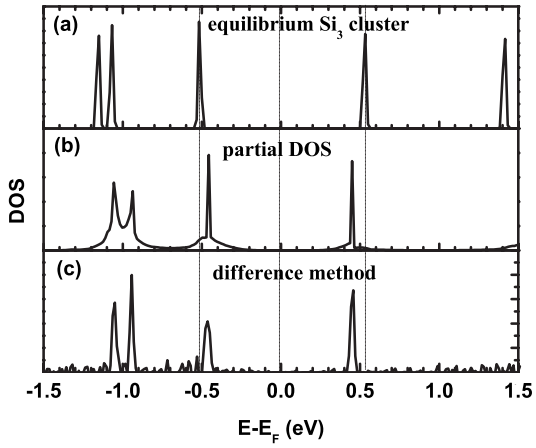


FIG. 8. Density of states (DOS) distributions for (a) the pure equilibrium $Si_3$ cluster, (b) the $Si_3$ cluster adsorbed on graphite from partial density of states (PDOS) calculation, and (c) the $Si_3$ cluster adsorbed on graphite by use of the difference method (see text).

markedly shifted with respect to those of the pure $Si_3$ DOS, documenting a distinct energy gap narrowing associated with the change from the pure to the adsorbed cluster of about 0.2 eV. Thus, even in the case of weak interaction between the substrate and the adsorbate, a pronounced decrease of the cluster energy gap is recorded, in keeping with the experimental trend.[6] About the same amount of energy gap narrowing is observed for the species $Si_n$ ($n=5-7$).

Investigating the energy gap change of $Si_n$ in response to adsorption on the diamond substrate, we find again a gap size reduction. Figure 9 contrasts the DOS of the pure $Si_5$ cluster with the PDOS of the cluster deposited on diamond. In the latter distribution, the peaks of the pure $Si_5$ cluster both undergo a shift of about 0.2 eV toward the Fermi level. The actual energy gap of $Si_5$ on diamond, however, is determined by the central PDOS maximum that appears at the midpoint of the energy gap, slightly below the Fermi level. This line is ascribed to substrate-adsorbate interaction. Taking into account the level broadening as may be assessed from Fig. 8,

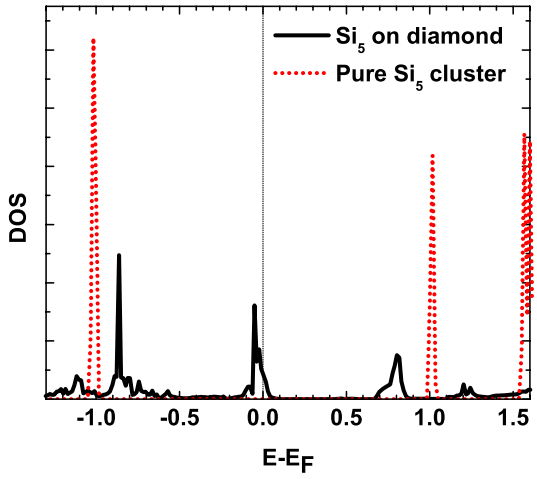


FIG. 9. (Color online) The DOS of the pure $Si_5$ cluster at equilibrium geometry and the PDOS of $Si_5$ adsorbed on diamond.

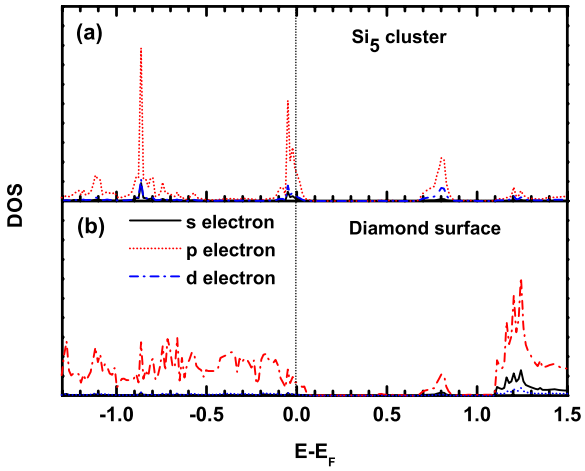


FIG. 10. (Color online) PDOS distributions of $Si_5$ (a) and of the diamond surface (b) for the combined system of $Si_5$ in contact with diamond.

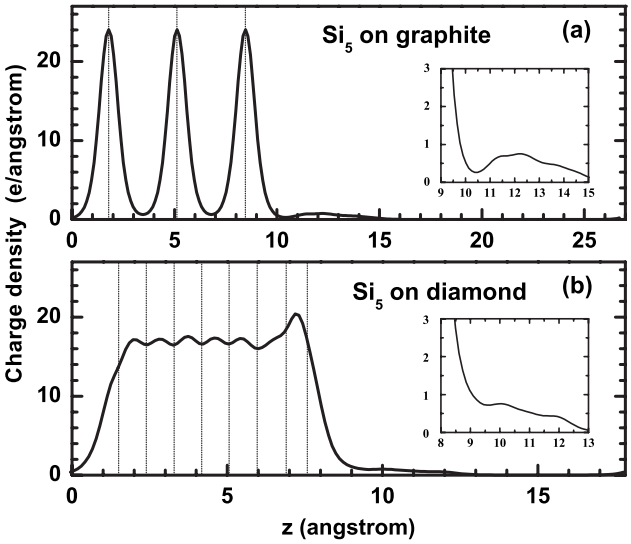


FIG. 11. The electron charge density distribution along the surface normal for the $Si_5$ cluster adsorbed on graphite (a) and diamond (b). The dotted lines indicate the positions of the substrate layers. The values shown were generated by integration over the lateral coordinates. The insets are for quantitative comparison of the electron charge density enhancement between the substrate and the attached side of $Si_5$ for graphite and diamond, reflecting the presence of covalent bonding between the cluster and the surface.

we estimate the resulting energy gap size as 0.6 eV.

For further analysis of the interaction between the clusters and the substrate, we plot the PDOS of the deposited $Si_5$ cluster and the diamond surface in Figs 10(a) and 10(b). The *p*-component is the most prominent contribution to the total DOS of the combined system. The $Si_5$ PDOS peak at 0.8 eV correlates with a small peak of the diamond surface PDOS. Likewise, the PDOS of the diamond surface in the interval $-1.0\ \text{eV} \leqslant E \leqslant -0.5\ \text{eV}$ is seen to correspond to a $Si_5$ PDOS continuum scattered around a dominant peak at $E = -0.85$ eV which has a less pronounced counterpart in the diamond distribution of Fig. 10(b). The $Si_5$ energy gap of approximately 0.6 eV matches that of the diamond substrate. The dramatic energy gap reduction of $Si_5$ upon deposition of the cluster on the diamond surface can thus be attributed primarily to the interaction between the *p* electrons of the substrate and the adsorbed cluster.

### H. Electron charge density distributions

Inspection of the electron charge density distributions adds a further viewpoint to the comparison between graphite and diamond as substrates for $Si_n$ deposition. In Fig. 11, the electron charge density is plotted as a function of the vertical coordinate (*z* direction) for the $Si_5$ cluster adsorbed on graphite [Fig. 11(a)] and diamond [Fig. 11(b)]. For the former, the electron charge density centers around the positions of the graphene layers. It does not vanish in the space between surface and the adsorbate. As we sum over the electron charge density of the $Si_5$ region, we detect no transfer of charge from $Si_n$ to graphite. Commenting on the $Si_5$-diamond system, the density is spread over the whole substrate region with peaks at the midpoints between adjacent layers and the highest density value coinciding with the maximum closest to the surface. This feature combined with the marked density reduction in the regime between the second and the third layer reflects a strong charge concentration at the diamond surface as a consequence of surface reconstruction. The distance between the second and the third layer is found to be about 0.2 Å larger than that of the diamond bulk [compare with Fig. 2(a)] which is ascribed to a lower electron charge density in this than in other interlayer regions. Sizable electron charge density, in contrast, is located in the interaction zone between the $Si_5$ cluster and the diamond substrate. In accordance with the discussion presented in Sec. III D, we associate the enhanced density above the surface layer with the bonding between substrate and adsorbate, involving the *p* electrons of both components. The insets in Fig. 11 allow for quantitative assessment of this effect for both substrates. Naturally, the electron charge density enhancement in the intermediate zone between the cluster and the substrate is drastically higher for diamond than for graphite, corresponding to much stronger covalent effects in the former than in the latter case.

## IV. CONCLUSIONS

The adsorption of Si atoms and small $Si_n$ clusters with $n=2-7$, on graphite and diamond substrates are studied by use of density functional theory within periodic boundary conditions. The results show that the deposition of $Si_n$ clusters on particle sites of graphite gives rise to adsorption structures of higher stability than that on the hole site. The bridge site turns out to be the most stable site for the adsorption of $Si_n$ clusters on diamond. Weak covalent bonding is found between the $Si_n$ clusters and the graphite substrate, while $Si_n$ and diamond interact much more strongly. There is no charge transfer from $Si_n$ clusters to the graphite substrate, in agreement with experimental results.[6]

The structural and electronic properties of the deposited $Si_n$ clusters are weakly affected by their interaction with the

graphite substrate, but considerably by the interaction with diamond. In particular, the energy gap of the $Si_n$ clusters shrinks due to the strong interaction between the $Si_n$ clusters and the diamond surface, as is demonstrated by comparison of the $Si_n$ PDOS distributions. While the energy gaps of $Si_n$ clusters reduce slightly due to their interaction with the graphite substrate, pronounced *p*-electron bonding effects lead to both a shift and a marked reduction of the $Si_n$ energy gap in the case of diamond, resulting in a gap size of about 0.6 eV. From a geometric point of view, the $Si_n$ clusters keep their gas phase equilibrium structures as they adsorb on graphite and undergo sizable deformation when deposited on diamond. The diamond substrate, in turn, reconstructs under the influence of the $Si_n$ adsorbate.

## ACKNOWLEDGMENTS

This work was supported by NSF Grant Nos. HRD-9805465, EPSCoR-440900 362427-02, and DMR-0304036, NIH Grant No. S06-GM008047, and the DoD through the U.S. Army/Engineer Research and Development Center (Vicksburg, MS) Contract No. W912HZ-06-C-0057.

[1] Z. Y. Lu, C. Z. Wang, and K. M. Ho, Phys. Rev. B **61**, 2329 (2000).
[2] D. Tománek and M. A. Schlüter, Phys. Rev. Lett. **56**, 1055 (1986).
[3] D. Tománek and M. A. Schlüter, Phys. Rev. B **36**, 1208 (1987).
[4] K. Raghavachari and V. Logovinsky, Phys. Rev. Lett. **55**, 2853 (1985).
[5] G. Pacchioni and J. Koutecký, J. Chem. Phys. **84**, 3301 (1986).
[6] B. Marsen, M. Lonfat, P. Scheier, and K. Sattler, Phys. Rev. B **62**, 6892 (2000).
[7] J. H. Wu, F. Hagelberg, and K. Sattler, Phys. Rev. B **72**, 085441 (2005).
[8] *Properties, Growth and Applications of Diamond*, edited by M. H. Nazar and A. J. Neves (The Institution of Engineering and Technology, Stevenage, UK, 2001).
[9] J. Furthmüller, J. Hafner, and G. Kresse, Phys. Rev. B **53**, 7334 (1996).
[10] G. Kresse and J. Hafner, Phys. Rev. B **47**, R558 (1993); **49**, 14251 (1994).
[11] G. Kresse and J. Furthmüller, Comput. Mater. Sci. **6**, 15 (1996).
[12] W. Kohn and L. J. Sham, Phys. Rev. **140**, A1133 (1965).
[13] N. D. Mermin, Phys. Rev. **140**, A1141 (1965).
[14] J. P. Perdew and A. Zunger, Phys. Rev. B **23**, 5048 (1981).
[15] H. J. Monkhorst and J. D. Pack, Phys. Rev. B **13**, 5188 (1976).
[16] D. M. Wood and A. Zunger, J. Phys. A **18**, 1343 (1985).
[17] P. Pulay, Chem. Phys. Lett. **73**, 393 (1980).
[18] P. E. Blöchl, Phys. Rev. B **50**, 17953 (1994).
[19] J. P. Perdew, K. Burke, and M. Ernzerhof, Phys. Rev. Lett. **77**, 3865 (1996).
[20] K. R. Kganyago and P. E. Ngoepe, Phys. Rev. B **68**, 205111 (2003).
[21] Y.-H. Kim, I.-H. Lee, S. Nagaraja, J.-P. Leburton, R. Q. Hood, and R. M. Martin, Phys. Rev. B **61**, 5202 (2000).
[22] F. Ortmann, W. G. Schmidt, and F. Bechstedt, Phys. Rev. Lett. **95**, 186101 (2005).
[23] P. E. Blöchl, O. Jepsen, and O. K. Andersen, Phys. Rev. B **49**, 16223 (1994).
[24] K. Rytkönen, J. Akola, and M Manninen, Phys. Rev. B **69**, 205404 (2004).
[25] Y. Jia, W. Zhu, E. G. Wang, Y. Huo, and Z. Zhang, Phys. Rev. Lett. **94**, 086101 (2005).
[26] C. Xiao, F. Hagelberg, and W. A. Lester, Phys. Rev. B **66**, 075425 (2002).
[27] A. Shvartsburg, B. Liu, M. F. Jarrold, and K. M. Ho, J. Chem. Phys. **112**, 4517 (2000).
[28] R. Jones, J. Phys. C **20**, L713 (1987).